LONG RANGE ACOUSTIC PROPAGATION OF HIGH FREQUENCY ENERGY IN THE INDIAN OCEAN FROM ICEBERGS AND EARTHQUAKES

Maya Tolstoy, DelWayne R. Bohnenstiehl and Emily Chapp

Columbia University

Sponsored by Air Force Research Laboratory

Contract No. DTRA01-01-C-0070

ABSTRACT

Naturally occurring sound sources are used to investigate the hydroacoustic propagation of high-frequency energy within the Indian Ocean Basin. These sources include tremor associated with ice movement along coastal Antarctica and moderate-to-large earthquakes associated with tectonic events adjacent to the Central Indian Ridge.

Ice-related signals, with variable spectral characteristics, are recorded throughout the year. The loudest of these ice events can be seen at both the Cape Leeuwin and Diego Garcia South hydroacoustic stations, with the arrivals at Diego Garcia South being attenuated at all frequency bands relative to Cape Leeuwin. The long-range propagation of these signals suggests that energy up to 90 Hz is coupling well through the convergence zone and into the SOFAR channel.

A specific type of ice-related signal, referred to as a 'cusped-pulsed', has been associated spatially with ice streams, which are rapidly flowing ice conduits that drain parts of the shelf into the sea. This identification was achieved through azimuthal and travel time calculations, and comparison of these location estimates with satellite imagery of the area. In addition, a more continuous harmonically-banded signal has been associated with a specific drifting iceberg (B-15D). The accuracy of these locations, as confirmed through satellite ground-truth data, suggests that ice-generated signals may yield a useful high-frequency acoustic source for future studies.

An extremely large (7.6 Mw) earthquake in the northwest Indian Ocean on July 15, 2003 [Bohnenstiehl *et al.*, 2004] has provided very intriguing data with regard to T-wave generation and long-range hydroacoustic propagation. Comparison of arrivals at Diego Garcia North, Diego Garcia South and Cape Leeuwin stations show a strong T-wave arrival at Diego Garcia North, a barely visible lower-frequency T-wave arrival at Diego Garcia South and a strong high-frequency arrival at Cape Leeuwin, despite apparent blockage along the direct path from much of the rupture plane to this station. Travel-time and azimuthal analysis suggests that the earliest T-wave arrival at Cape Leeuwin consists of converted P- and S-wave energy sourced from the eastern scarp of the Chagos and Maldives Archipelagos, at distances of several hundred kilometers from the earthquake rupture. The highest-frequency and highest-amplitude component of the Cape Leeuwin T-wave signal packet exhibits an arrival time consistent with a dominantly hydroacoustic path that may be partially refracted through a bathymetric low to the north of Diego Garcia or represent T-wave energy scattered in the near-field from the region adjacent and to the north of the main rupture. Reflections from bathymetric highs to the north and east of the rupture zone are evident within the T-wave coda.

OBJECTIVES

Propagation of high-frequency energy through the Antarctic Convergence Zone (ACZ) is a poorly understood problem. However, understanding this process is an important problem in signal discrimination. In particular, the high-latitude regions of the southern ocean lack a SOund Fixing And Ranging (SOFAR) channel, and so there has been considerable concern that energy generated in these areas would not be readily detectable using IMS hydrophone stations. Our objectives were to look for signals that could be used to study propagation through the ACZ, as well as studying high-frequency blockage associated with shallow bathymetric features.

Utilizing primarily hydroacoustic data from Diego Garcia South and Cape Leeuwin we have studied the origin of ice-related signals with high-frequency energy and their propagation through the ACZ and over thousands of kilometers through the Indian Ocean SOFAR channel. Utilizing hydroacoustic data from the Diego Garcia North, Diego Garcia South and Cape Leeuwin hydroacoustic stations (Figure 1) we have studied the high-frequency blockage of a particularly large (7.6 Mw) earthquake that showed unusual propagation of low and high frequency energy through areas where significant blockage would have been expected.

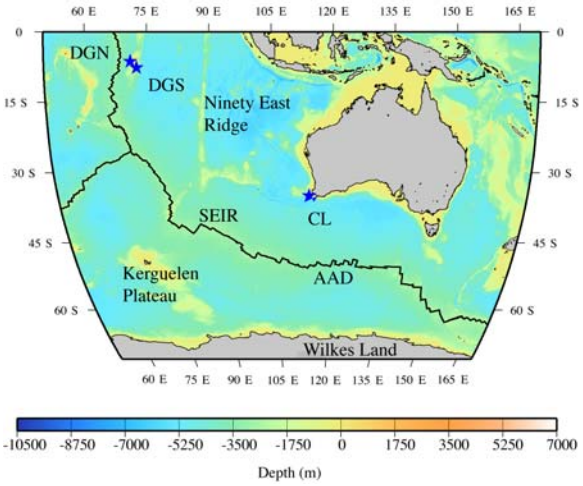

Figure 1. Map of Indian Ocean Basin study area. Blue stars indicate hydrophone triad locations labeled as CL (Cape Leeuwin), DGS (Diego Garcia South) and DGN (Diego Garcia North. Mid-ocean ridges shown as black lines with the following geographic location labels: Southeast Indian Ridge (SEIR), Australian-Antarctic Discordance (AAD), Ninety East Ridge, Kerguelen Plateau, Wilkes Land section of Antarctica. Color bar indicates sea floor bathymetry in meters relative to sea level.

RESEARCH ACCOMPLISHED

Propagation of Ice-Related Signals through the Convergence Zone

Variable Harmonic Tremor (VHT)

The dominant tremor type observed at the DGS and CL stations consists of multiple harmonic bands with spectral peaks that fluctuate in frequency through time, hereinafter referred to as Variable Harmonic Tremor (VHT) (Figure 2). These tremors are comparable to the iceberg-related signals observed by Talandier *et al.* [2002] at lower-frequencies (< 25 Hz) using Pacific Seismic Network (PSN) seismic stations. Our sound-channel based observations indicate a fundamental frequency that is typically within the 4-10 Hz range (Figure 2a,b panel 5), but can reach as high of 30 Hz in some instances (Figure 2c, panel v). As many as eight spectral bands can be seen in some tremor packets, with significant power above 80 Hz (Figure 2b). VHT signal packets can persist from ~ 1-30 min, but their occurrence is spatially clustered with periods of activity lasting from hours to days.

As illustrated in Figure 2 (panels i and ii), VHT signals commonly exhibit abrupt starts and stops, and in some instances these polychromatic signals evolve from or into a continuous monotonic signal (Figure 2b) or broadband noise (Figure 2a,b,c). Within a signal packet, azimuth estimates do not change significantly through time, despite changes in the spectral character of the signal (Figure 2a,b,c, panel 3). This suggests that these various portions of the signal packet likely originate from the same source region or within a narrow source zone. The received signal strengths of the VHTs at DGS range from 119-133 dB re 1µPa and those at CL range from 126-142 dB re 1µPa (peak-to-peak). Signals were seen throughout the year; however, many of the loudest and longest duration signals were observed during the Austral fall and winter.

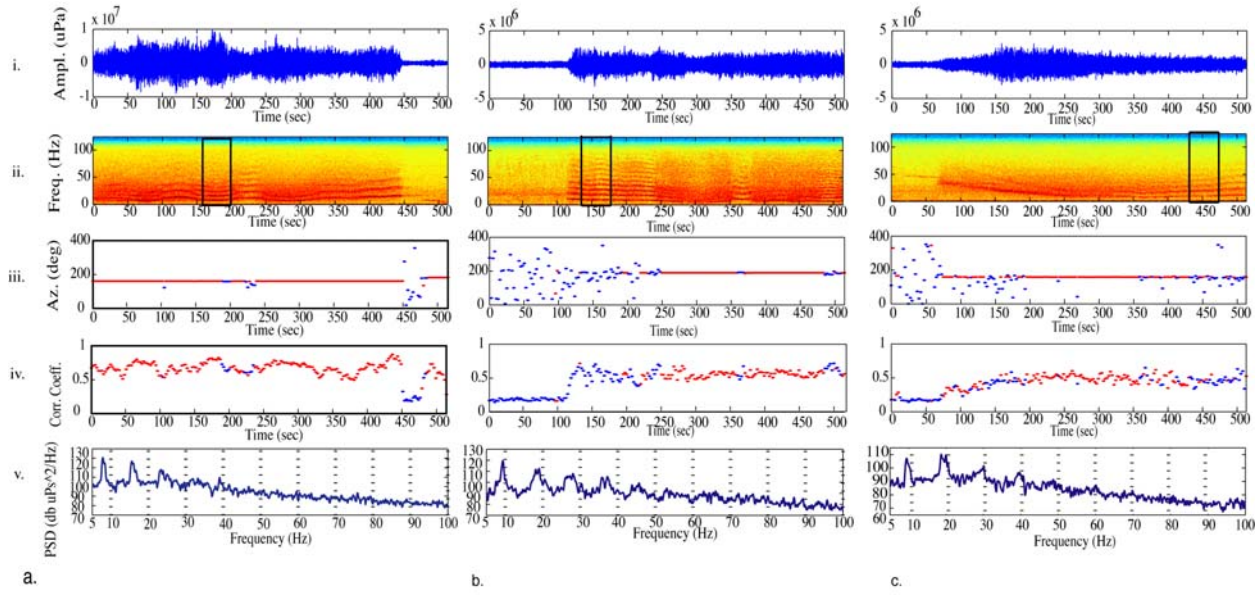

Figure 2. (a, b, c) Signal (i), spectrogram (ii), azimuth (iii), correlation coefficient of azimuth calculation (iv), and power spectral density plots (v) of three different VHT signals recorded on CL hydrophones in 2002, Julian Day (JD) 113 at 12:36; 2003, JD 128 at 23:31; and 2002, JD 208 at 04:19, respectively. Note the harmonic bands of energy with fundamental frequency at ~ 7, ~ 9, and ~ 8 Hz, respectively and the variation in spectral content as each signal progresses with time. Red dots on the azimuth and correlation coefficient panels represent points where the slowness velocity was 1.485 ± 0.03 km/sec. The abrupt onset and termination of these signals are typical of VHTs. Azimuth calculations used a bandpass filtered (5 to 35 Hz) signal using 5 second windows with 50% overlap, and power spectral density plots used the boxed portion of the spectrogram (45 second window) using zero padding and a Hanning window.

In keeping with the observations of Talandier *et al.* [2002], a subset of the loudest VHT episodes can be correlated spatially and temporally with a large (~8 x 27 km) iceberg that migrated westward along the eastern Antarctic coast during 2002 and early 2003 (Figure 3). This iceberg, B-15D, was originally calved from the same ice mass that spawned the B-15B iceberg tracked by Talandier *et al.* [2002] within the Ross Sea. The azimuths for six pairs of VHT signals that were recorded at both the CL and DGS stations are shown in Figure 3a, with shaded areas representing error bounds for each signal. Satellite-derived iceberg locations, color-coded in time, show the westward migrating iceberg B-15D. As iceberg positions are not updated daily, we have used iceberg locations within three days of the VHT arrivals. For each episode, B-15D locations fall within the error bounds of our azimuthal locations.

The set of possible locations that satisfy the differential arrival time (Δt) data for stations CL and DGS are shown in Figure 3b. These curves also show reasonable agreement with the B-15D locations that are temporally closest to the time of the VHT observations. A constant velocity medium of 1.475 km/s provided the best agreement between the locations derived from the intersection of the azimuth pairs (Figure 3a) and the differential arrival time locations, with the absolute value of the residuals being between 1 and 29 seconds.

Most of the VHT azimuths, however, do not align with drifting icebergs. Figure 4 shows azimuthal paths and locations calculated for the VHT signals from 2002 through mid-2003, with green and red lines representing azimuths calculated from CL and DGS, respectively. The prevalence of these signals suggests that VHT noises may be generated by smaller icebergs, which are not being tracked, but litter the Antarctic shelf region, or that VHT signals can be generated also by coastal ice sources. The Wilkes Land region, for example, is populated by a number of outlet glaciers and ice streams, which are distributed throughout the region where azimuthal data indicate the VHT signals originate (Figure 4). As the ice scrapes over the bedrock, harmonic signals could be generated in a manner analogous to an iceberg scraping the shelf. Consistent with this idea, Talandier *et al.* [2002] have identified

at least two tremor episodes not associated with drifting icebergs in January 2001 and November 2000 that appear to originate from the Mertz Glacier (~68°S, 145° E) and the Tucker Glacier (~72°S, 170° E), respectively. Our data shows the area near the Mertz glacier to be very active in 2002 and 2003 with several VHT azimuths aligning with this section of the coast. A direct hydroacoustic acoustic path does not exist, however, between the hydrophone stations and the Tucker glacier within the Ross Sea region.

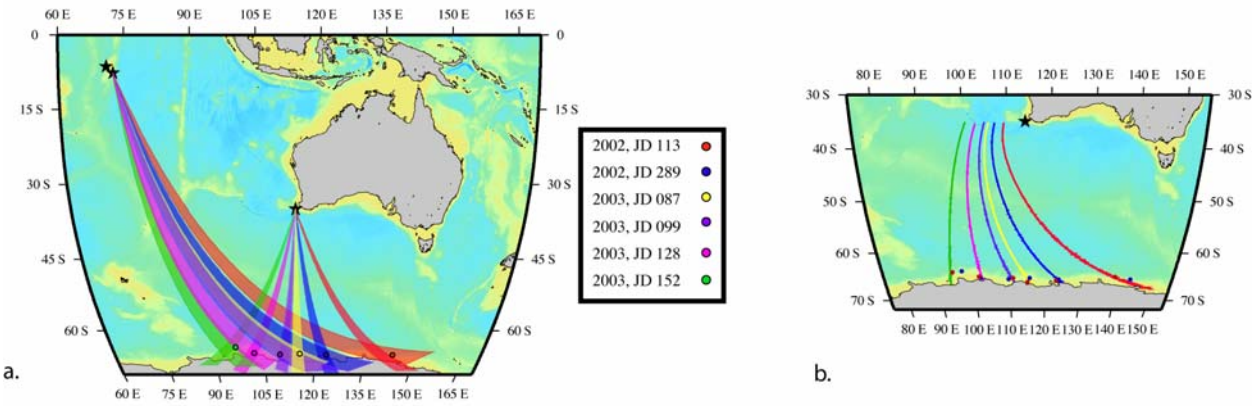

Figure 3. a.) Azimuths of six VHT signals from CL and DGS hydrophones along with iceberg locations. Each colored circle represents the National Snow and Ice Data Center (NSIDC) location of iceberg B-15D at various times throughout 2002 and 2003 (steady westerly migration). Each colored path corresponds to the azimuth and error bounds (±1.26 degrees for CL and ±1.51 for DGS derived from known earthquake locations) calculated from signals arriving at CL and DGS hydrophones within 3 days of the NSIDC reported locations. Black stars represent hydrophone locations. b.) Differential travel time curves for each of the six VHT signals. Each curve represents a set of locations yielding the calculated arrival time differences using a 2 km by 2 km spaced grid and a sound velocity of 1.475 km/sec. Red dots indicate our iceberg locations derived from azimuths, and dark blue dots indicate NSIDC locations.

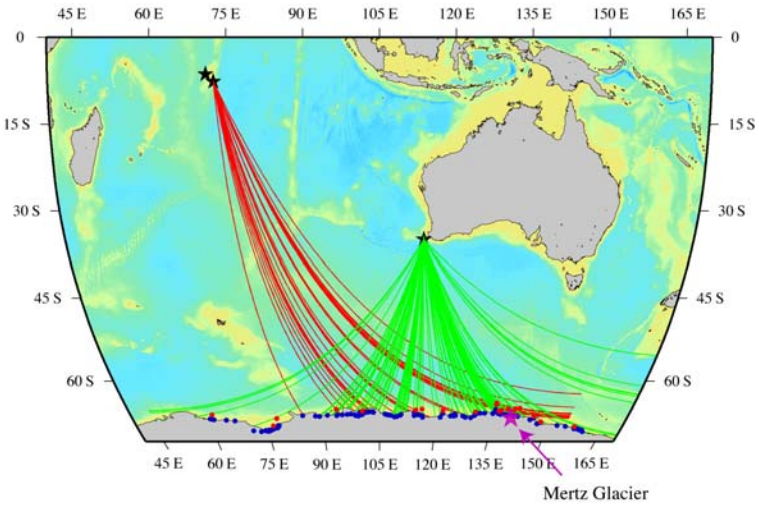

Figure 4. Azimuth traces for VHT signals recorded on CL hydrophones (green) and DGS hydrophones (red) in 2002 and 2003. Blue dots indicate USGS named glaciers, red dots indicate locations for glacial tongues, and black stars represent hydrophone locations. Note the gaps between azimuth paths where no glaciers and ice streams are present. The deficiency in azimuths falling west of 90°E are a result of partial blockage from the geography of the Antarctic coast and the Kerguelen Plateau, and an absence of azimuths east of 160°E may reflect the limits of our detection capabilities. There are a small number of easterly CL azimuths (>150 degrees) that appear to originate from lower latitudes for which we have no explanation.

Cusped-Pulsed Tremor (CPT)

A second signal, a cusped-pulsed tremor (CPT) signal, is characterized by curved harmonic bands of energy in the 4-100 Hz frequency range with fundamental frequencies ranging from 4-10 Hz (Figure 5). The CPT signals were only seen on 31 days in 2002 and on 7 days in 2003 (up to May 2003), occurring primarily in the Austral fall and winter. The received levels of these signals range from 126-139 dB re 1 μPa at CL and 120-131 dB re 1 μPa at DGS. There appearance is very similar to some hydroacoustically-observed volcanic tremor [e.g., Dziak and Fox, 2002], with the duration of a single pulse ranging from 25-60 sec and the interval between pulses ranging from 30-90 sec. Pulsed signal trains can last anywhere from 10 min to over 1 hr. They usually exhibit a near regular pulse spacing (Figure 5a); however, some series have pulses at variable intervals (Figure 5b).

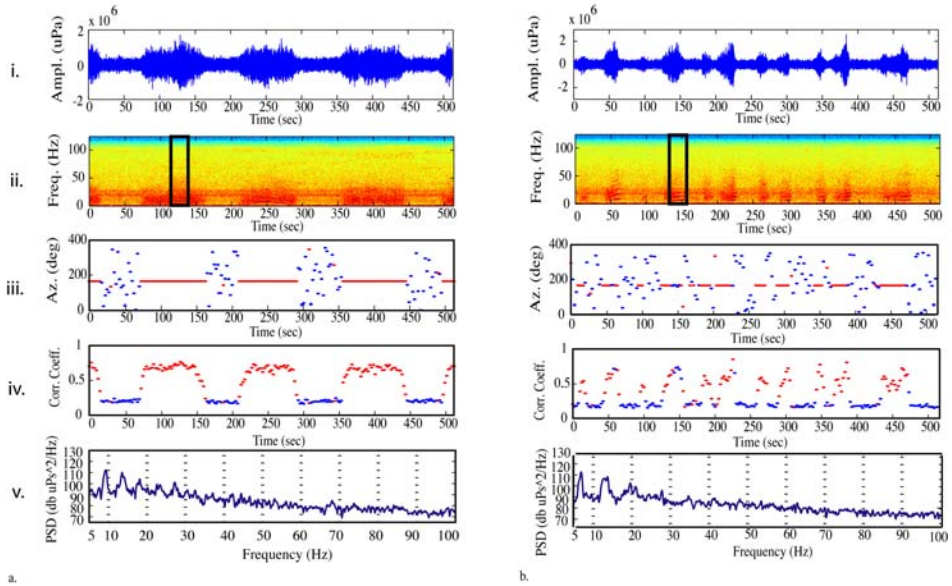

Figure 5. (a and b). Signal (i), spectrogram (ii), azimuth (iii), correlation coefficients of azimuth (iv), and power spectral density plot (v) of pulses in a regularly spaced CPT series (a.) and an irregularly spaced CPT series (b.) recorded on CL hydrophones starting at 2002, JD 160 at 11:07 and 2002, JD 177 at 20:43 respectively. The fundamental frequencies of the series are ~ 9 and ~ 6 Hz with harmonics up to at least 35 Hz. Red dots on the azimuth and correlation coefficient panels represent points where the slowness velocity was 1.485 ± 0.03 km/sec. Azimuth calculations used a bandpass filtered (5 to 35 Hz) signal using 5 second windows with 50% overlap, and power spectral density plots used the boxed portion of the spectrogram (20 second window) using zero padding and a Hanning window.

Azimuth calculations show fixed azimuths throughout each pulse, as well as the entire pulse series (Figure 5, panel iii), with pulses exhibiting high correlations coefficients. Unlike the more continuous VHT signals there is no coherent energy between the pulses (Figure 5, panel iv).

CPT azimuthal locations were checked against iceberg locations from the NSIDC. While icebergs were present within the error bounds of a few signals, the majority of the signals did not originate from known iceberg locations. Moreover, those CPT signals that did have icebergs near their azimuth track were observed later in the year originating from the same location after the iceberg had drifted out of the error bounds—suggesting that the sources for the CPT signals remain fixed.

Unlike the VHT azimuths that included most of the Antarctic coast from 90°E to 160°E, CPT signals only originate from five geographic areas. CPT azimuths are shown in Figure 6a with green and red lines representing azimuths calculated from both CL and DGS, respectively. RADARSAT imagery from the source regions, as estimated from intersecting azimuth pairs, show small ice streams in each of these areas. Free floating ice blocks are observed trailing off some of these ice streams, perhaps indicative of ongoing activity. Figure 6b shows sets of possible CPT

source locations based on the arrival time differences between the CL and DGS stations. Each curve falls within the errors of our azimuth calculated source locations, with the absolute values of Δt residuals ranging from 0.6-47 sec.

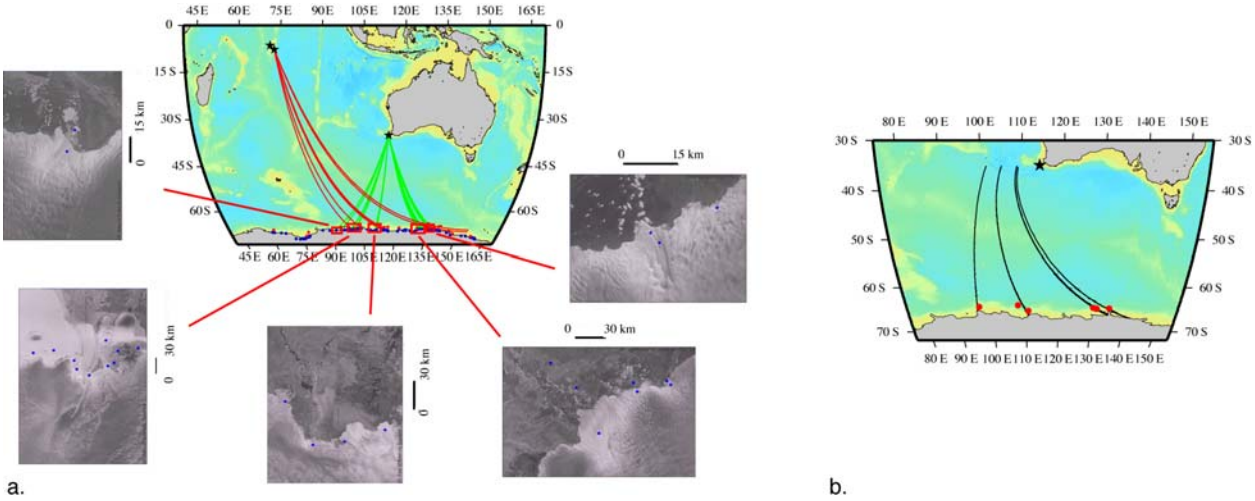

Figure 6. a.) Azimuth traces for CPT signals recorded on CL hydrophones (green) and DGS hydrophones (red) in 2002 and 2003. Blue dots indicate USGS named glaciers, red dots represent glacier tongue locations, and black stars represent hydrophone locations. The red squares show areas where RADARSAT images are taken and the figures around the map are the corresponding satellite images. Blue dots on the images are the same glacier locations as those on the map. Note the presence of several different ice streams connecting the glaciers to the ocean, some with floating blocks of ice trailing from the ends of the streams, which may be indicative of on-going activity. b.) Differential travel time curves for the CPT series where DGS data produced reasonable azimuths. Each curve represents a set of locations yielding the calculated arrival time differences using a 2 km by 2 km spaced grid and a sound velocity of 1.475 km/sec. Red dots indicate the CPT locations for each travel time curve. Note some curves overlap for different CPT locations.

Discussion

The spatial and temporal correlations outlined above argue that the observed tremors are generated in association with drifting icebergs and coastal ice sources, such as outlet glaciers and ice streams. Similarities between the VHT signals described here and ice-related signals reported by Talandier et al. [2002] argue strongly for a common source mechanism. Talandier et al. [2002] have suggested that harmonic nature of the Ross Sea tremors results from resonance with a drifting iceberg or fluid filled cavity within the iceberg. As seafloor scours appear to be common within many polar shelf regions and the icebergs became acoustically quiet after leaving the shelf, they argued that this resonance is excited as the iceberg scrapes the seafloor.

The dominant 4-10 Hz fundamental observed within the VHT signals is consistent with the observations of Talandier et al. [2002]; however, in some instances, these hydroacoustic data show fundamental frequencies exceeding 30 Hz (Figure 2). If similar high-frequency energy was generated during the Ross Sea tremor events, those signals would have been aliased by the PSN seismic sensors—as would many of the high-order overtones in Figure 2. Talandier et al. [2002] have discussed possible types of resonators in some detail. As they point out, the lowest frequency ~3 Hz fundamentals would corresponded to the eigenfrequency of a vertical shear mode within a ~300 m thick ice layer (assuming β=1.8 km/s). This thickness is consistent with that predicted for iceberg B-15, and sufficient to allow the ice mass to scrape across portions of the shelf. Higher-frequency fundamentals (~10-30 Hz) would suggest resonance within an ice layer having a thickness of only a few tens of meters. Other possible resonator scenarios include the excitation of a fluid (water and air) filled cavities within the ice, making the eigenfrequency a complex function of the cavity's shape and size, as well as the impedance contrast between the fluid and surrounding ice mass. Changes in these parameters during ice movement could help to explain spectral fluctuations during the tremor events [Talandier et al., 2002].

Despite the correlation of some VHT signals with a large iceberg being tracked by the NSIDC, our observations suggest that tremor signals also may be linked to the movement of smaller icebergs and/or coastal ice sources along eastern Antarctica. The land-based portion of glacial ice masses and their glacial tongues are known to be active in many areas. These ice tongues extend over the water where they can break up into smaller blocks of ice that could become mobile due to the influence of wind and waves [Menzies et al., 1995]. As with larger drifting icebergs, acoustic signals generated within or near these tongues could radiate energy into the water column.

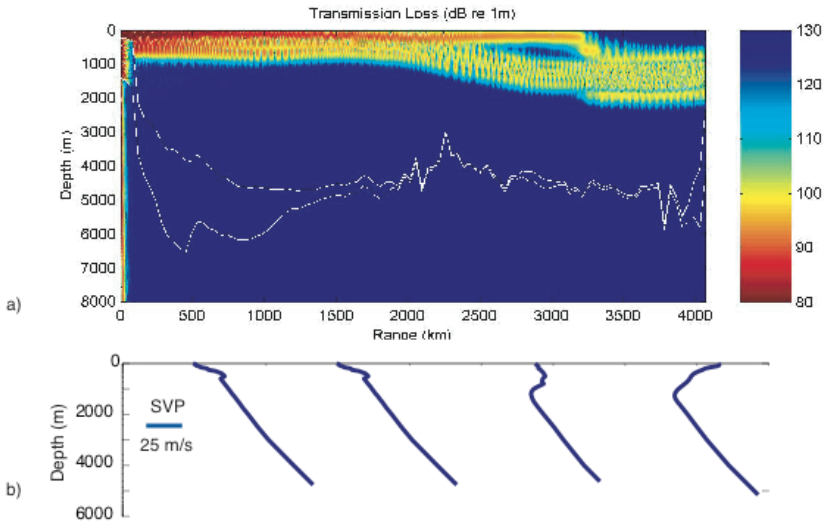

Figure 7. a) Transmission loss model for a 40-Hz source at a depth of 100 m near the Mertz Glacier (~86 S, 145 E). The Cape Leeuwin receiver is located at a depth of 1100 m at a range of ~4100 m. Range dependant sediment thickness is derived from a NOAA sediment thickness database and range dependant sound velocity profiles are taken from the US Navy's Generalized Digital Environmental Model (GDEM) for the month of July (30 minute resolution). Sediment properties: 1600 m/s sound speed, density 1.5 g/cm^3,compressional attenuation of 0.15 dB/m/kHz. Bottom properties: 2300 m/s sound speed, density 2.21 g/cm^3, compressional attenuation of 0.05 dB/m/kHz. The PE code UMPE2DBB was used in this calculation [Smith, 2001]. b) Sample sound velocity profiles along the transect.

The abrupt onset and termination of many of the VHT signals (Figure 2) suggests the ice is moving in stick-slip manner, and there is mounting evidence for such behavior in within Antarctic glaciers and ice streams. For example, a continuous GPS study recently demonstrated tidally influenced stick-slip motion within a Siple Coast ice stream in western Antarctica. Individual slip events lasted from 10 to 30 minutes with an average slip velocity of ~1 m/hr [Bindschadler *et al.*, 2003]. This duration is similar to the VHT signals observed in the IMS hydroacoustic data, and the surging nature of the ice movement could act to excite these tremor signals. Similarly, Ekstrom *et al.* [2003] have identified a series of unusual long-period surface wave events (equivalent to a > 4.5 M earthquake) located in glacial regions, including tectonically stable areas such as Greenland and coastal Antarctica. As opposed to a standard double-couple earthquake source model, the radiation pattern of these events could be modeled as a single force couple, as previously applied to landslides. This led the authors to suggest that these events were generated by stick-slip glacial quakes.

Although CPT signals are observed to originate from a subset of the active ice streams within the Wilkesland region, the environmental conditions necessary to generate these signals are not well constrained. The near uniform spacing of CPT signals is reminiscent of a geyser-like process, as observed within subareal volcanic systems. Consequently, we speculate that the process may be hydrologically driven, with a periodic recharge that allows the glacier to slip in a repeating manner. It is not clear why some ice streams generate CPT signals and others do not.

In high latitude regions, colder oceanic temperature profiles do not facilitate the existence of a deep sound channel. Acoustic energy from a shallow depth source along the Wilkesland shelf must initially propagate as a surface reflected phase, crossing the Antarctic convergence zone, and later becoming coupled within the mid-latitude sound

channel. In Figure 7, a parabolic equation (PE) code [Smith, 2001] is used to investigate propagation from a source near the Mertz Glacier. This model confirms that sound propagation from Antarctica is still possible in the absence of a SOFAR channel and that energy can be transferred efficiently into the sound channel, where the IMS hydrophones are moored. Transmission loss estimates using this model for a path to CL are ~100 dB, implying maximum source levels of more than 240 dB re 1μPa @ 1 m.

Blockage of High Frequency energy from Earthquake Sources

On July 15, 2003, an extremely large (7.6 Mw) earthquake occurred in the northwest Indian Ocean [Bohnenstiehl *et al.*, 2004]. Comparison of arrivals at Diego Garcia North, Diego Garcia South and Cape Leeuwin stations shows a strong T-wave arrival at Diego Garcia North, a barely visible lower-frequency T-wave arrival at Diego Garcia South and a strong high-frequency arrival at Cape Leeuwin (Figure 8), despite apparent blockage along the direct path from much of the rupture plane to this station. This large event, along with its well-located aftershocks, allows some interesting observations to be made regarding blockage.

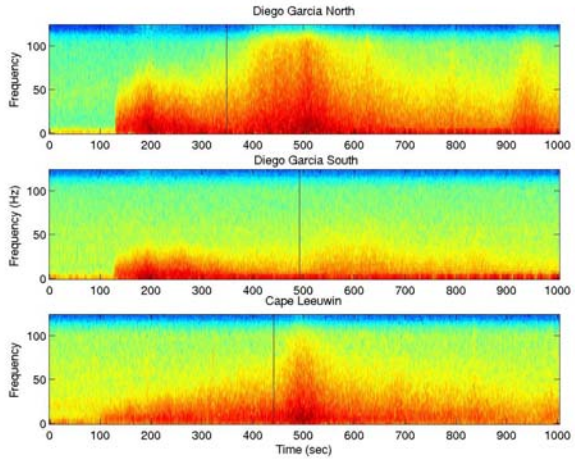

Figure 8. Spectrogram for earthquake arrival at Diego Garcia North (top), Diego Garcia South (middle), and Cape Leeuwin (bottom). Thin vertical black line indicates predicted start time of T-wave arrival. Abrupt P-wave arrivals are evident at both Diego Garcia stations. Cape Leeuwin shows a prolonged build up of energy before the primary T-wave.

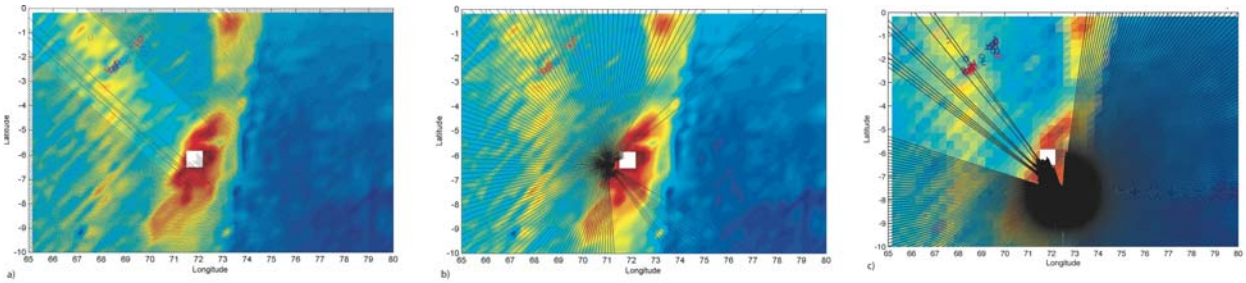

Figure 9. Blockage maps with 50 m stop criteria and 1 degree rays for Cape Leeuwin (a), Diego Garcia North (b) and Diego Garcia South (c). Red circles – detected aftershocks. Blue circles – not detected aftershocks. White square – Diego Garcia.

Figure 9 shows blockage maps for all three stations with a 50-m cut off, and earthquake locations color coded to indicate if they were observed (red) or not (blue) at the given station. The maps show that the 50-m cut off is a fairly good indication of when signals will be blocked. However, those observed signals that traveled over relatively shallow areas were quite weak and lacking in high-frequency energy.

The strike-slip mainshock event ruptured ~ 210 km of crust, with an estimated rupture duration of ~ 65 seconds. T-wave azimuths from arrivals at Diego Garcia North indicate that the bulk of the T-wave energy was generated at the moment centroid location, which is consistent with that being the location of the maximum earthquake energy release.

Arrivals at Cape Leeuwin, particularly for the mainshock provide some surprising results. Travel-time and azimuthal analysis suggest that the earliest T-wave arrival at Cape Leeuwin consists of converted P- and S-wave energy

originating from the eastern scarp of the Chagos and Maldives Archipelagos, at distances of several hundred kilometers from the earthquake rupture. Figure 10 shows the varying azimuth associated with the long T-wave arrival at Cape Leeuwin, along with predicted arrival azimuths and times for P-wave and S-wave energy from the epicenter, moment centroid and end of rupture for a variety of bathymetric features (Figure 11).

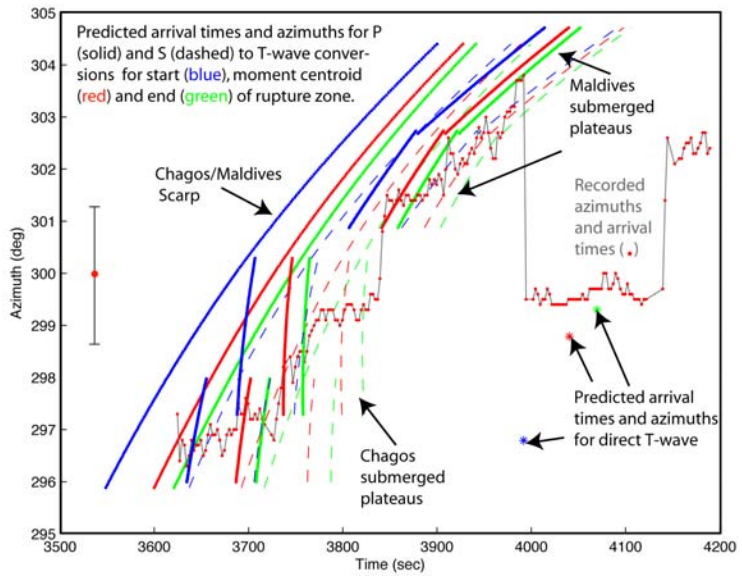

Figure 10. Calculated azimuths (red dots) for the T-wave arrival at Cape Leeuwin (see Figure 8 – bottom) compared with predicted arrival times and azimuths for P-wave (solid lines) and S-wave (dashed lines) that converted to T-waves on various bathymetric features of the Chagos and Maldives Archipelagos (see Figure 11). Predictions are made for energy coming from the start of the rupture (blue), the centroid moment (red) and the end of the rupture (green). Also shown are predicted arrival times and azimuths for the direct T-wave arrival (*). Note last set of azimuths (~4150-4200 seconds) may indicate a reflected arrival from the more northern features on the Maldives Archipelago.

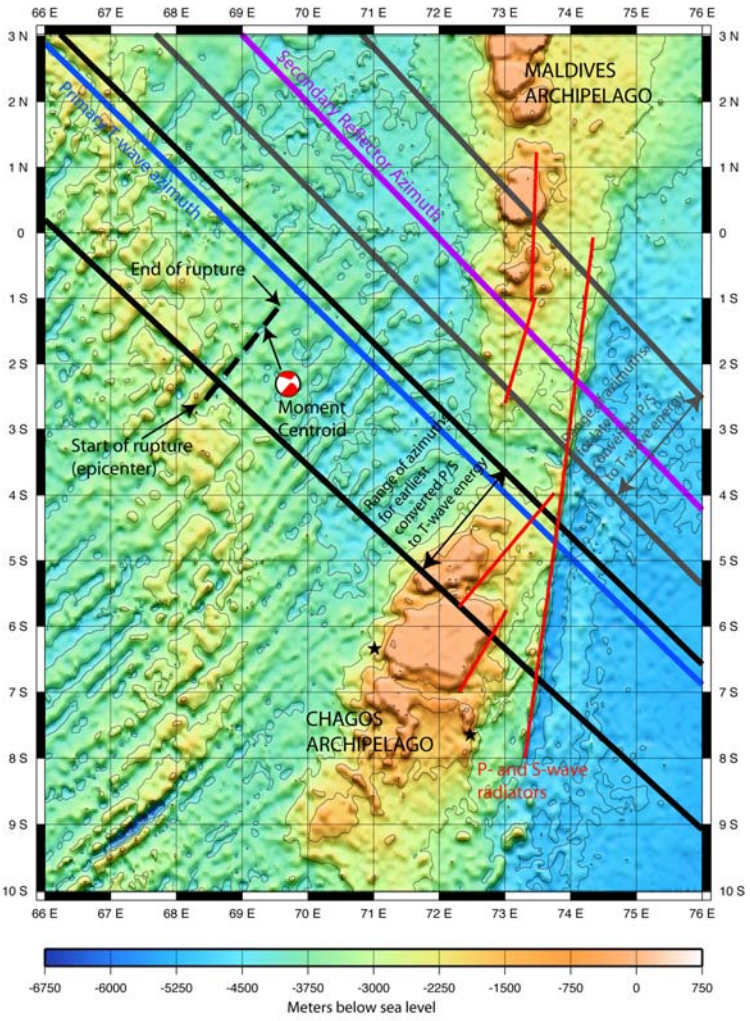

Figure 11. Primary bathymetric features associated with Cape Leeuwin T-wave arrival from July 15th, 2003 7.6 Mw earthquake. Earthquake rupture area is indicated by the dashed black line with the start, moment centroid, and end positions noted. Black and gray lines indicate the range of azimuths for converted P/S-wave to T-wave energy observed for the earlier and later arrivals respectively (see Figure 10). Red lines indicate likely radiators, with arrival times modeled in Figure 10. The blue and purple lines indicate azimuths for the primary high frequency direct T-wave arrival and a later reflected arrival respectively.

The direct T-wave energy, which arrives at a time consistent with an exclusively water-borne pathway, comes in at an azimuth a little to the north of the end of the rupture, and aligned with a deeper area between the Chagos and Maldives Archipelagos. It appears therefore that the energy was either refraction around the northern area of the Chagos bathymetric highs, or that it represents significant excitation of the seafloor north of the actual rupture zone. The latter is reasonable given the magnitude of the earthquake and the relative roughness of the seafloor adjacent to this slow spreading ridge segment. This arrival is the only portion of the T-wave train that contains significant high-frequency energy. Lower energy reflections from Maldives bathymetric highs to the north and east of the rupture zone are evident within the T-wave coda and show azimuths consistent with the Maldives submerged plateaus.

CONCLUSIONS AND RECOMMENDATIONS

We have characterized two hydroacoustic sources capable of exciting high-frequency energy that propagates over 8000 km through the Indian Ocean. From hydroacoustic data, azimuth calculations and satellite imagery, we have defined surging ice streams and drifting icebergs as the dominant signal generators along the coastal sections of Wilkesland, eastern Antarctica. The harmonic nature of these signals supports the idea of resonating ice masses, and the calculated azimuths allow specific areas of active ice movement to be located. These naturally occurring sources provide excellent tools for more details studies of long-range propagation of high-frequency energy through the ACZ.

To better utilize these natural sources, ground-truthing of source locations and near field characterization of the signals should be accomplished through hydrophone measurements made within 10-100's of km of the source, well within the ACZ. Utilizing such tools would allow individual sources to be well located, and provide an improved source model for use in investigating propagation across the ACZ.

Our studies of hydroacoustic blockage support the idea that T-wave energy can be generated from multiple scatters. It also appears that high frequency energy generated by near-field scattering from the seafloor may be detected, even though the direct path may be partially or completely blocked. This scattered energy represents the highest frequency, highest amplitude portion of the arrival for the July 15, 2003 mainshock. While blockage appears fairly complete for smaller events when bathymetry of < 50 m is encountered, some energy is still transmitted at relatively shallow depths > 50 m. Further rigorous analysis of large earthquake sources of opportunity would help confirm these observations, and provide more detailed understanding of the processes.

REFERENCES

Bindschadler, R.A., M.A. King, R. B. Alley, S. Anandakrishnan, and L. Padman, (2003) Tidally controlled stick-slip discharge of a West Antarctic ice stream, *Science*, 301, 1087-1089.

Bohnenstiehl, D.R., M. Tolstoy, and E. Chapp (2004), Breaking into the Plate: A 7.6 Mw Fracture Zone Earthquake Adjacent to the Central Indian Ridge, *Geophys. Res. Lett.,* 31, doi:10.1029/2003GL018981.

Dziak, R.P., and C.G. Fox (2002), Evidence of harmonic tremor from a submarine volcano detected across the Pacific Ocean basin, *J. Geophy. Res.,* 107, 10,1029-10,1044.

Ekstrom, G., M. Nettles, and G.A. Abers (2003), Glacial earthquakes, *Science,* 302, 662-624.

Menzies, J. (1995),The dynamics of ice flow, in: J. Menzies (Ed.), Modern Glacial Environments: Processes, Dynamics and Sediments, Buterworth Heinemann Ltd., Oxford, 139-196.

Smith, K.B. (2001), Convergence, stability, and variability of shallow water acoustic predictions using a split-step Fourier parabolic equation model, *J. Comp. Acoust.,* 9, 243-285.

Talandier J., O. Hyvernaud, E.A. Okal, and P.-F. Piserchia (2002), Long range detection of hydroacoustic signals from large Icebergs in the Ross Sea, Antarctica, *Earth and Planet. Sci. Let*., 203, 519-534.